Chem. Eur. J. **2004**

Supporting Information

for

"Stabilizing or Destabilizing Oligodeoxynucleotide Duplexes Containing Single 2'-Deoxyuridine Residues with 5-Alkynyl Substituents"

by
Thomas Kottysch, Carolin Ahlborn, Frank Brotzel, and Clemens Richert

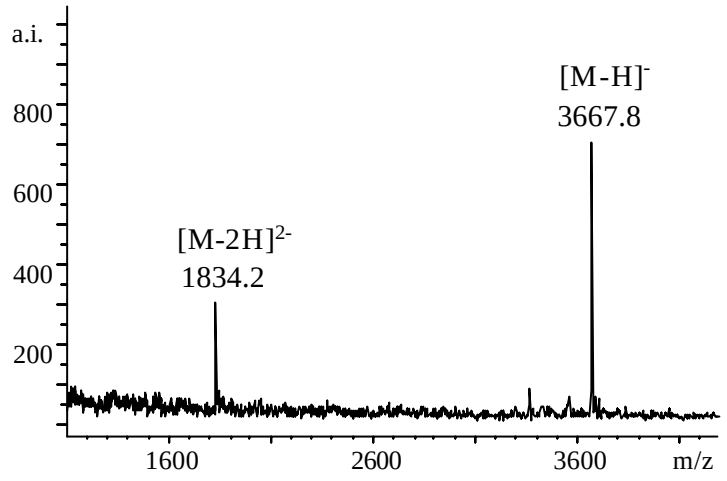

Figure S1. MALDI-TOF mass spectrum of **19a**.

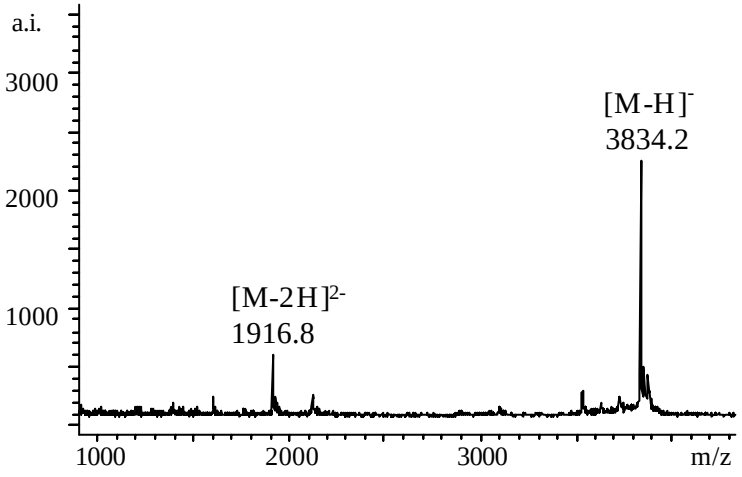

Figure S2. MALDI-TOF mass spectrum of **19b**.

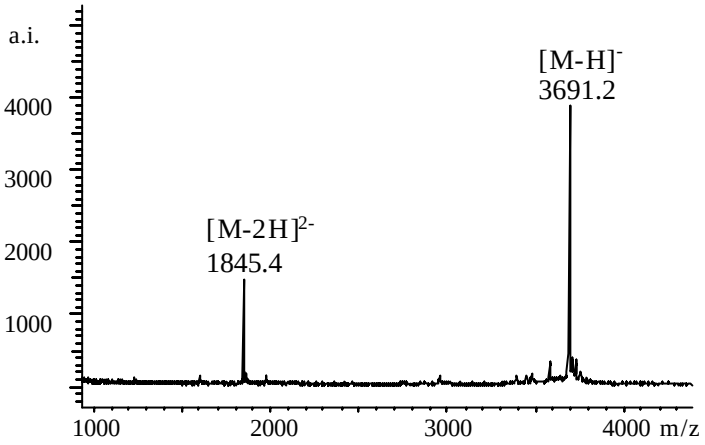

Figure S3. MALDI-TOF mass spectrum of **19c**.

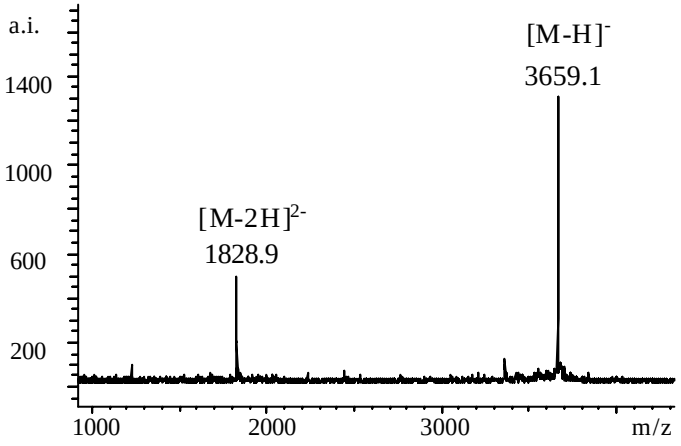

Figure S4. MALDI-TOF mass spectrum of **19d**.

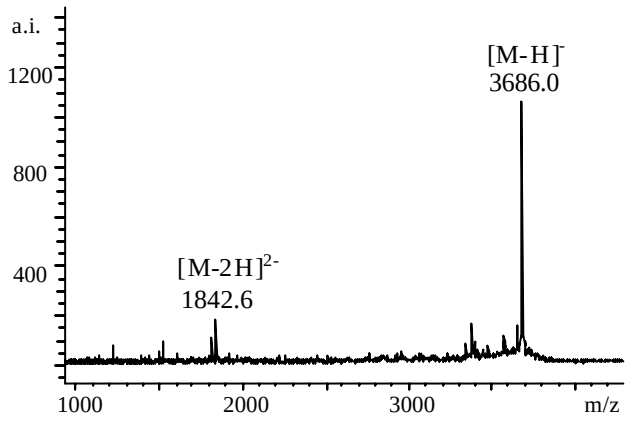

Figure S5. MALDI-TOF mass spectrum of **19e**.

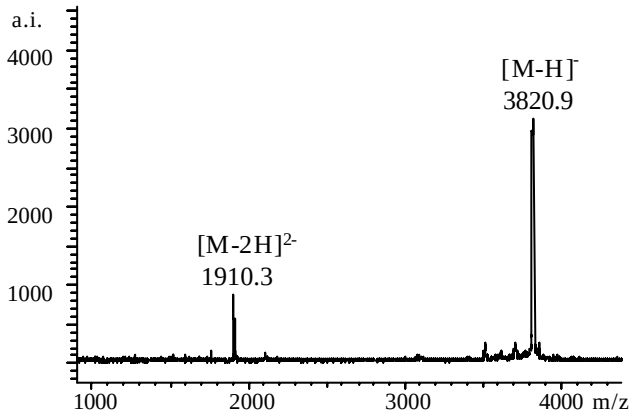

Figure S6. MALDI-TOF mass spectrum of **19f**.

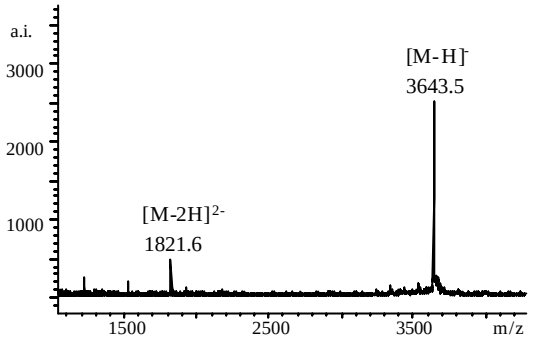

Figure S7. MALDI-TOF mass spectrum of **19g**.

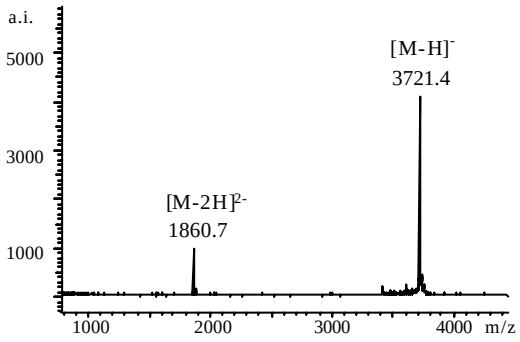

Figure S8. MALDI-TOF mass spectrum of **19h**.

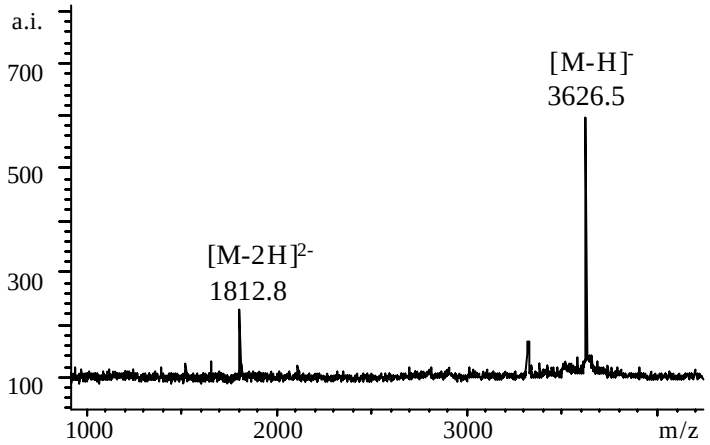

Figure S9. MALDI-TOF mass spectrum of **19i**.

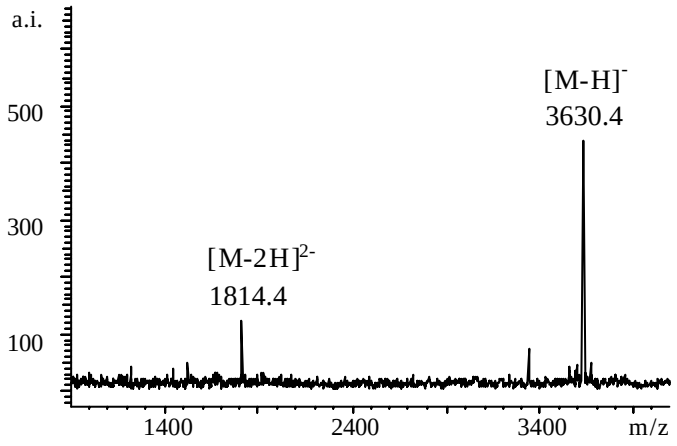

Figure S10. MALDI-TOF mass spectrum of **19j**.

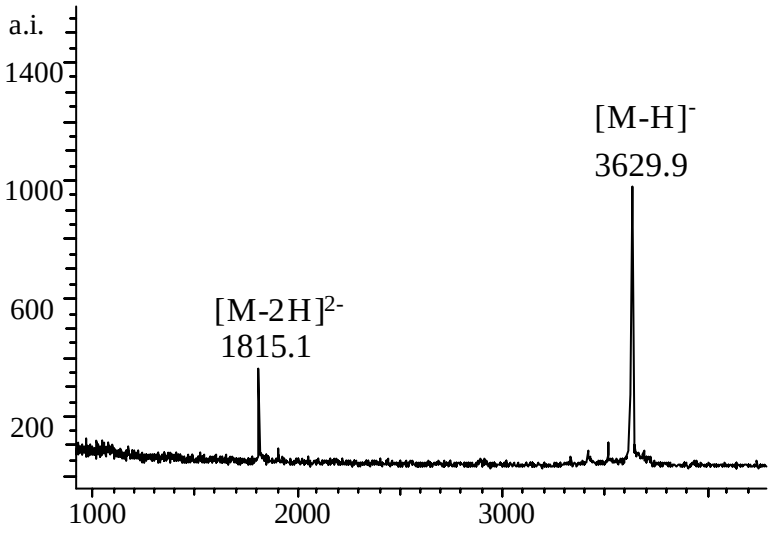

Figure S11. MALDI-TOF mass spectrum of **19k**.

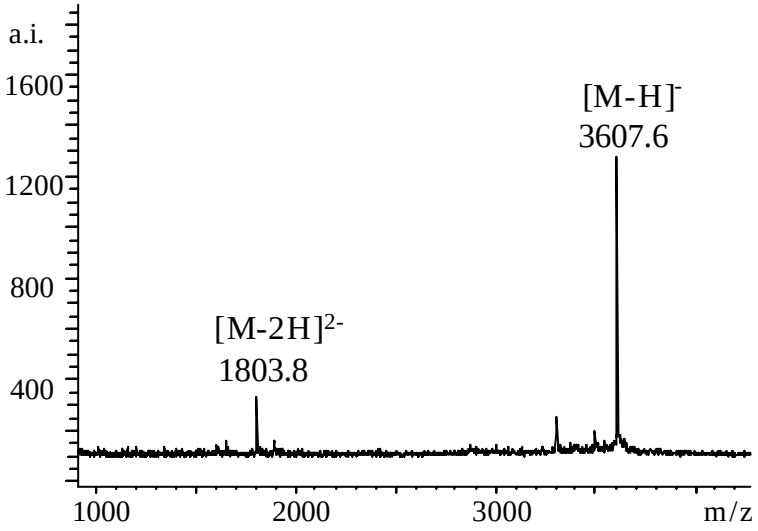

Figure S12. MALDI-TOF mass spectrum of **19l**.

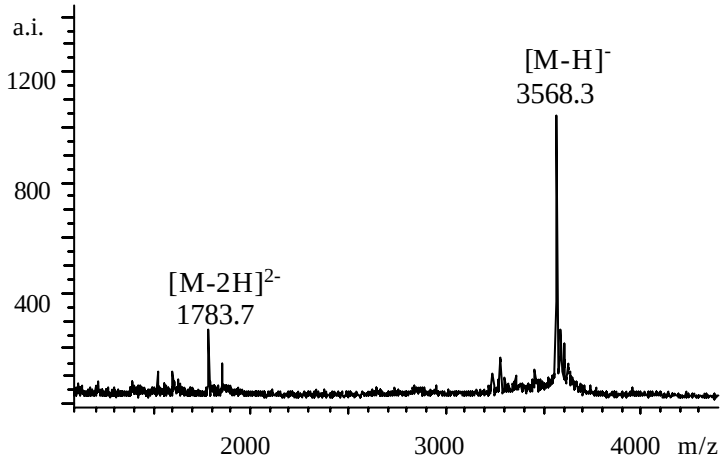

Figure S13. MALDI-TOF mass spectrum of **19m**.

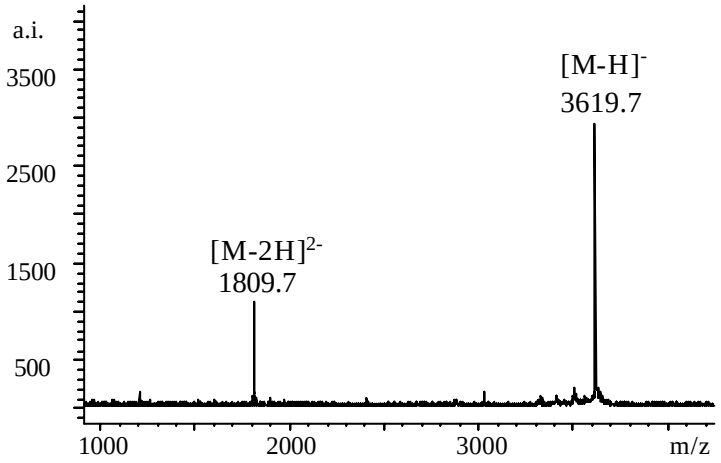

Figure S14. MALDI-TOF mass spectrum of **19n**.

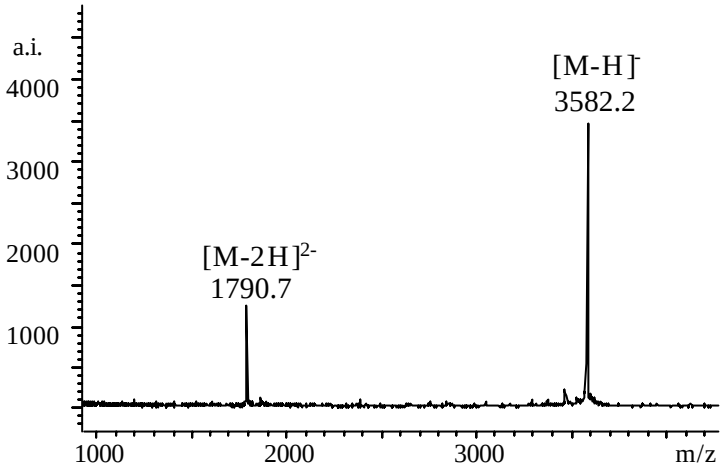

Figure S15. MALDI-TOF mass spectrum of **19o**.

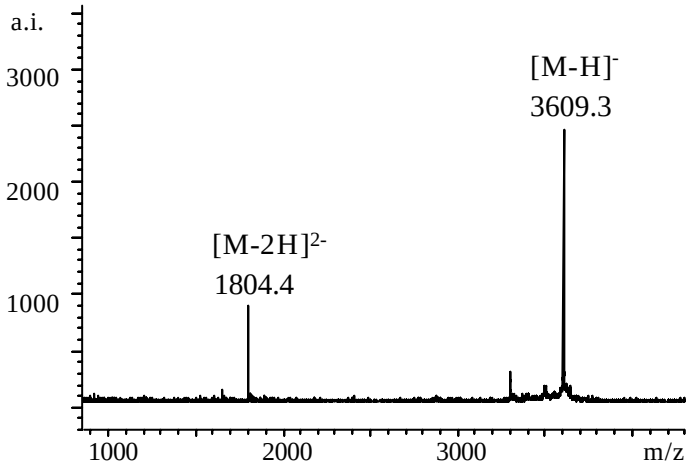

Figure S16. MALDI-TOF mass spectrum of **19p**.

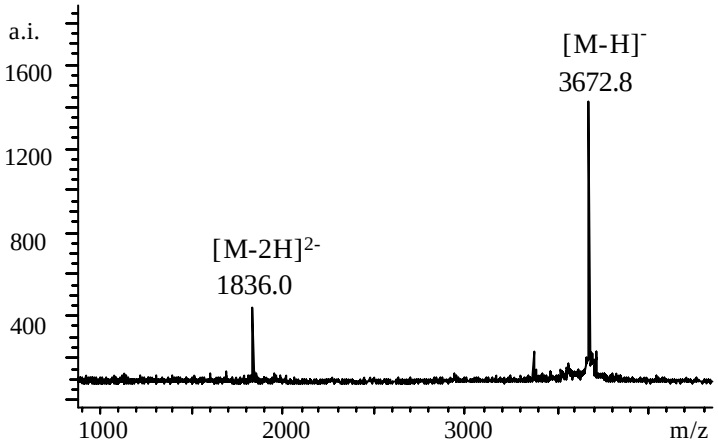

Figure S17. MALDI-TOF mass spectrum of **19q**.

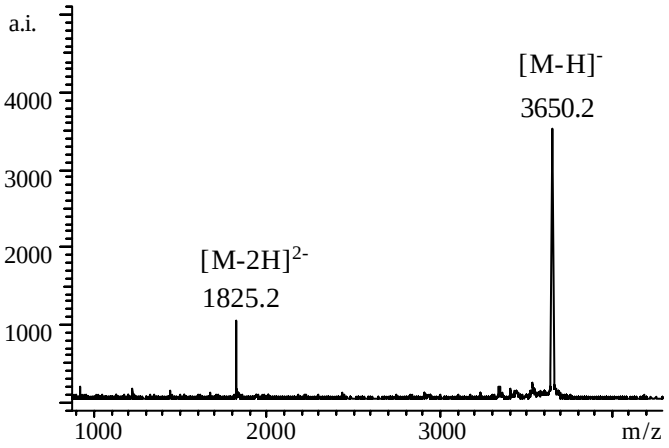

Figure S18. MALDI-TOF mass spectrum of **19r**.

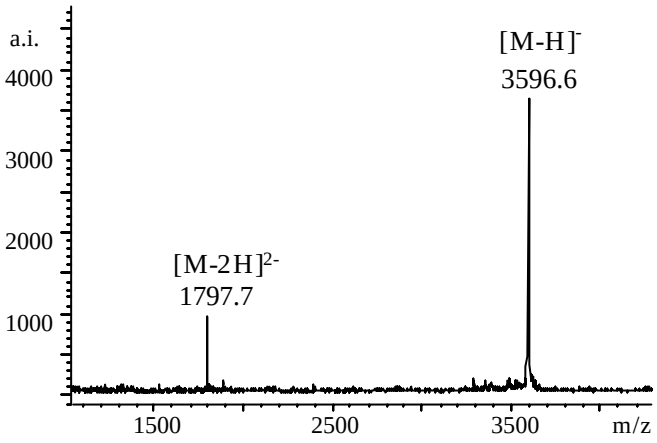

Figure S19. MALDI-TOF mass spectrum of **19s**.

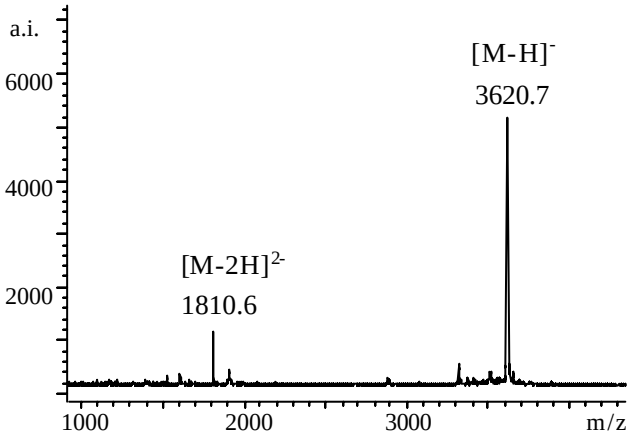

Figure S20. MALDI-TOF mass spectrum of **19t**.

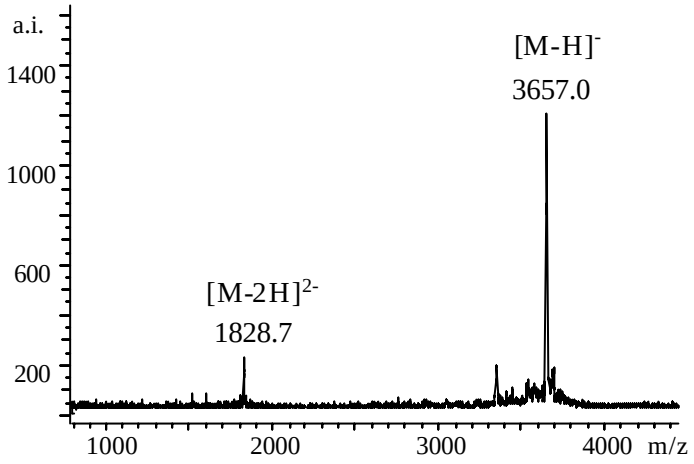

Figure S21. MALDI-TOF mass spectrum of **19u**.

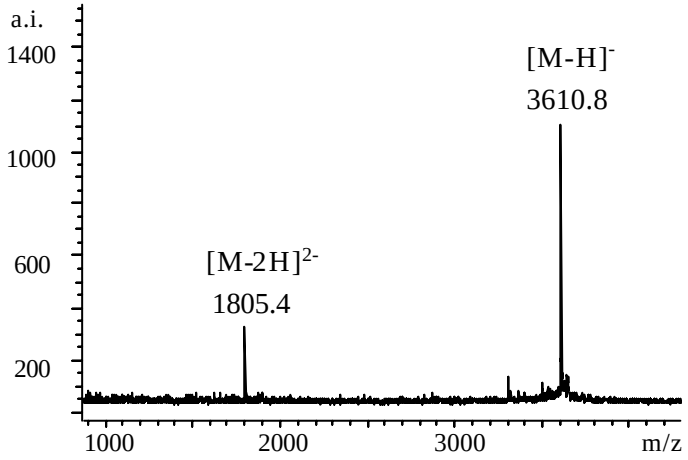

Figure S22. MALDI-TOF mass spectrum of **19v**.

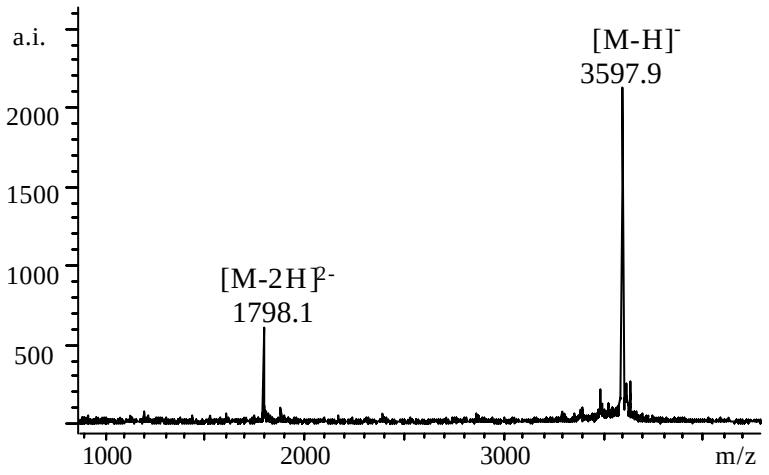

Figure S23. MALDI-TOF mass spectrum of **19w**.

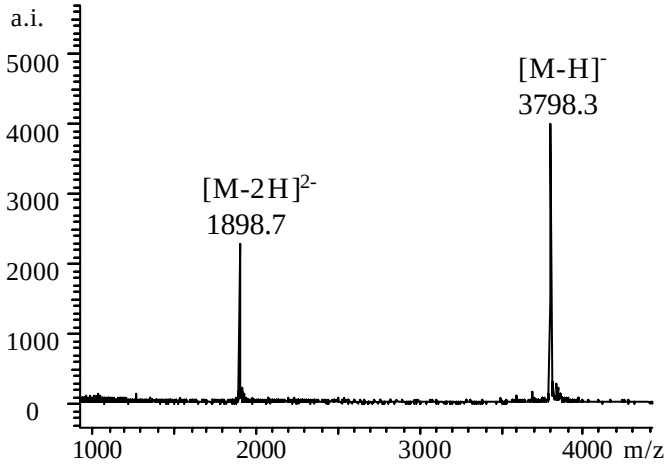

Figure S25. MALDI-TOF mass spectrum of **19y**.

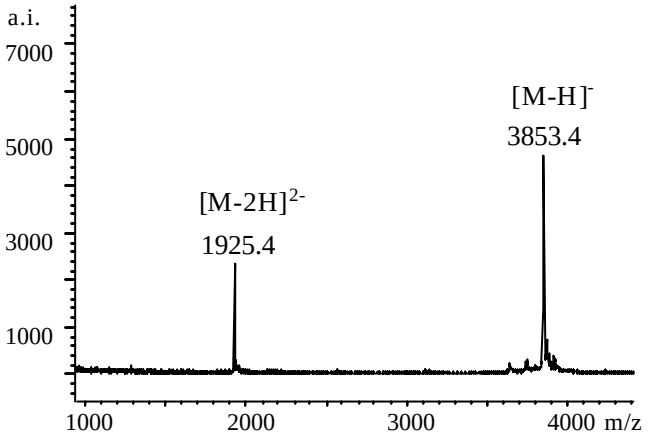

Figure S24. MALDI-TOF mass spectrum of **19z**.

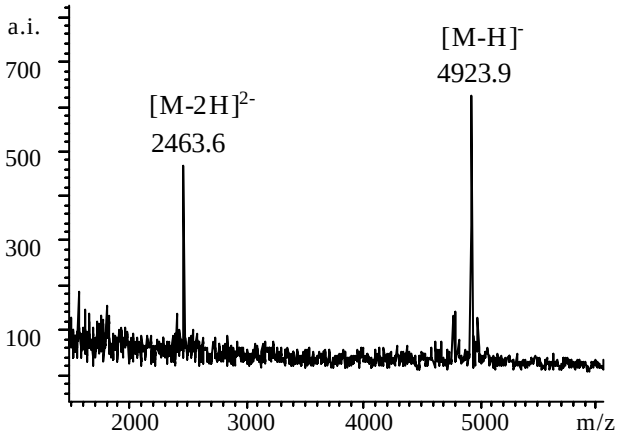

Figure S26. MALDI-TOF mass spectrum of **30**.

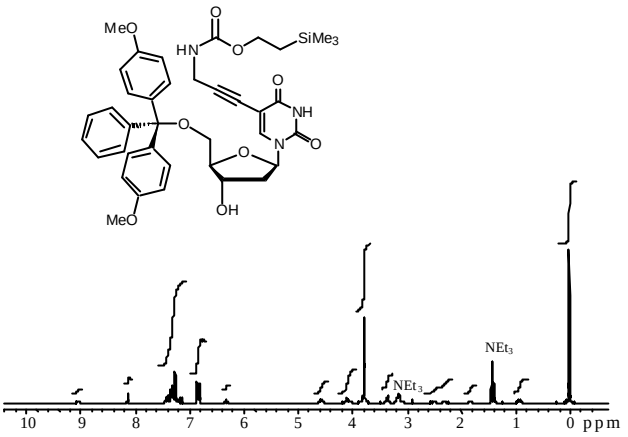

Figure S27. ^{1}H-NMR spectrum (250 MHz, $CDCl_3$) of **5**.

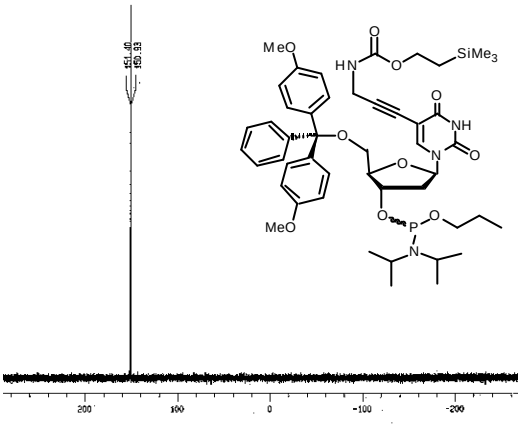

Figure S28. ^{31}P-NMR of **1** (101 MHz, DMSO-d_6).

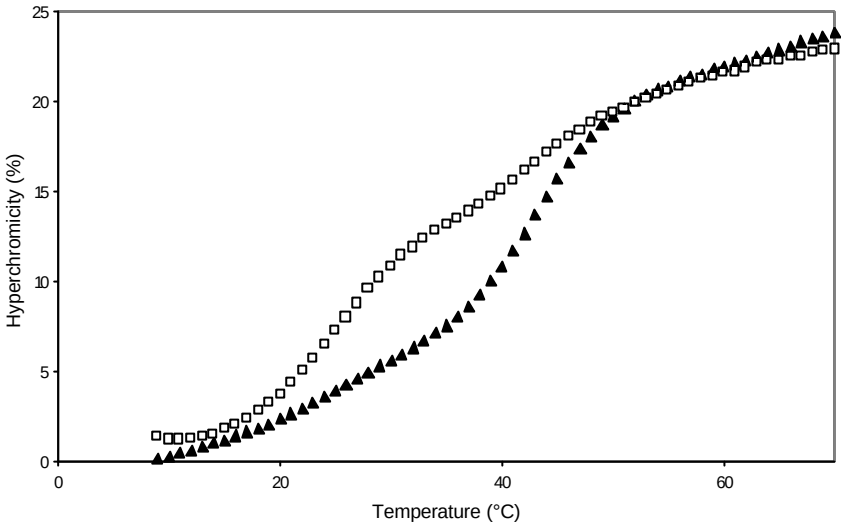

Figure S29. UV-melting curves for the duplex **19a**:**14**, obtained at *1M* salt, as defined in Table 1. Melting curves from two independent experiments with two independently synthesized samples are shown. Both were acquired in the heating mode (from low to high temperature). The curves shown are the most divergent results obtained for a total of eight melting experiments. It can be discerned that the relative intensity of the two transitions differs, but the respective melting points are close to invariant. Since some hysteresis was observed between individual curves, and melting curves starting at a higher temperature showed less of the first transition, it is possible that the kinetics of formation for the structure whose melting underlies the low temperature transition are slower than usual for DNA duplexes.